Jurnal Fizik Malaysia Volume 39 Issue 2 (2018) pgs 20001-20012 A. Ghoshal

Resonances in Positronic Lithium under Quantum Plasmas

Arijit Ghoshal[a] and Yew Kam Ho[b]

[a]*Department of Mathematics, Burdwan University, Golapbag, Burdwan 713 104, West Bengal, India*
[b]*Institute of Atomic and Molecular Sciences, Academia Sinica, P.O. Box 23-166, Taipei, Taiwan 106*
[a]*arijit98@yahoo.com*

(Received: 28.1.2018 ; Published: 7.6.2018)

Abstract. The stabilization method (SM) is employed to look into the low-lying resonances in positronic lithium (e^+Li) embedded in quantum plasmas (QP). Screened interaction in QP is described by the Debye-Huckel cosine potential (DHCP). Two resonances have been found to appear below the Ps(n=2) excitation threshold ($E_{th}^{Ps(2)}$). Energy and the width of those resonances are determined by calculating the density of resonance states. It is seen that the position of the resonances is gradually pushed towards the Ps(2s) with increasing plasma screening strength. For the unscreened case, our reported results are in close accord with other reliable results available in the literature. To the best of our knowledge, the present results will be the first reported results of resonance in e^+Li under QP.

Keywords: positron, lithium, resonance, stabilization method, quantum plasma.

I. INTRODUCTION

Investigations on the structural and collisional properties of atomic systems embedded in quantum plasmas have received considerable attention in the recent years [1–25], mostly because of the existence of these plasmas in various physical situations, such as in astrophysical bodies [26, 27], in plasma experiments [28, 29, 30], in nano-scale objects [31–37]. A distinctive feature of quantum plasmas is that they are relatively cool and dense, such as their temperature T and density N_e lie around $10^2 - 10^5$K and $10^{24} - 10^{29}$m^{-3} [38] respectively. If, in a plasma, the de Broglie wavelength of the charge carriers becomes comparable to the dimension of the plasma system, the quantum mechanical effects play a key role in determining the collective behavior of charged plasma particles [39]. This might happen if a plasma is sufficiently cooled. QP can consists of electrons, positrons, ions and charged nano-particles. In comparison to the classical plasmas, which generally obey Maxwell-Boltzmann distribution, quantum plasmas obey the Fermi-Dirac statistical distribution.

Due to the shielding effect of plasma the interactions among the charged particles in an atomic system embedded in a plasma will be modified. This modification leads to substantial changes in the structural properties of an atomic system. The shielding or screening of potential in a plasma can be approximated adequately by a model potential which is subject to

the temperature and density of the underlying plasma. On assuming that the quantum force acting on the electrons dominates over the quantum statistical pressure, Shukla and Eliasson [40] have proved that the field of potential of a test charge of mass m implanted in QP can be modelled by the Debye-Huckel cosine potential (DHCP) or the exponential cosine-screened potential (ECSCP) of the form (in a.u.):

$$V(r) = -\frac{1}{r}e^{-r/\kappa_D}\cos(r/\kappa_D), \tag{1}$$

where κ_D is related with ω_p (plasma frequency) and k_q (quantum wave number) by the relation $\kappa_D = \sqrt{(\hbar\omega_p/m)}/\omega_p = \sqrt{2}/k_q$. $\mu_\kappa(=1/\kappa_D)$ is known as the plasma screening parameter.

In this paper, our aim is to investigate the low-lying resonances in e^+Li embedded in QP. In particular, we look into the S-wave resonances appearing below the $E_{th}^{Ps(2)}$. Positronic lithium (e^+Li) is the atom formed by the attachment of a positron to a lithium atom [41]. The atom is electronically stable against the disassociation into both the $Li-e^+$ and Li^+-Ps channels, but not against electron-positron annihilation [42]. In vacuum, the ground state energy of e^+Li is -0.002484 a.u. [42]. In fact, attachment of a positron to a neutral atom or molecule to form a bound (or a quasi-bound) state is a matter of great concern and has been the subject of extensive studies for the last two decades [42–62] (and further references therein). The emergence of resonance states connected with excited states of atom in the positron scattering spectrum, or connected with an excited positronium atom interacting with the Li^+ ion [53], serves as a signature of binding of positron to that atom. Moreover, the appearance of such low-lying S-wave resonances may give rise to a resonant radiative recombination (RRR) process [63], which is sure to occur in dense plasma.

In a recent investigation, Ghoshal and Ho [43], using the SM, identified two resonance states lying below the $E_{th}^{Ps(2)}$ in e^+Li embedded in classical Debye plasma (DP). Screened interaction of the charged particle was represented by Debye-Huckel potential (DHP) of the form (in a.u.):

$$V(r) = -\frac{1}{r}e^{-\mu_\lambda r}, \tag{2}$$

where $\mu_\lambda = \omega_P/v_T$ is the plasma screening parameter with v_T as the plasma thermal velocity. The lowest resonance was found to survive for longer screening strength than the other. In this paper, our endeavour is to study how those resonance states are affected by the quantum behaviour of the background plasma. Such a study is very significant, because it has been seen that plasmon excitation spectrum of Dirac fermions gets appreciable change, when collective quantum diffraction effect is considered in graphene [64]. Furthermore, the effect of electron-exchange is also important in the formation of the screened interaction in degenerate QP [65]. It is thus anticipated that an atomic system in QP can behave in a significantly different way from what is observed in classical DP. It muat be mentioned that the screening parameters μ_λ and μ_κ, ascribed to the screening models ([1] and [2]), respectively, carry somewhat different physical sense. However, for the sake of discussion, henceforth the same notation μ will be used to represent the screening parameter for both QP and DP.

II. METHODS AND CALCULATIONS

In the present paper, our approach to determine resonances in e^+Li is two-folded - the application of the method of model potential (MMP) to treat Li atom as consisting of a frozen core along with a valence electron, followed by the application of the SM to determine the resonance parameters (RP). MMP is an effective method to deal with a multi-electron atom in a convenient way. In this method, the lithium atom is regarded as a two-body system comprising of a positive ionic core (Li^+) and an electron (active). The core includes the effects of the passive electrons. The interaction potential between the ionic core and the electron is then obtained in such a way that it corresponds to the exact binding energies of the atom. The MMP has been explored in detail earlier [66–70], and a number of model potentials (MP) are available in the literature to present Li atom in vacuum. In the present investigation, the interaction potential between the Li^+ core and the active electron in QP is represented by the following MP (in a.u.):

$$V_M^{(e^-)}(\vec{r}_2) = -\frac{e^{-\mu r_2}}{r_2}\cos(\mu r_2)\left[1+2(e^{-2\alpha r_2}+\beta r_2 e^{-2\gamma r_2})\right], \tag{3}$$

where $\vec{r}_2$ is the coordinate of the active electron relative to the core (assumed to be infinitely heavy), and α, β, γ are parameters to be determined. To determine α, β and γ we solve the eigen value problem of the corresponding Hamiltonian $h_1 = -\frac{1}{2}\nabla_2^2 + V_M^{(e^-)}(\vec{r}_2)$ with the framework of the Rayleigh-Ritz variational principle by employing the following trial wavefunction:

$$\phi = \phi_{nlm}(\vec{r}_2) = R_{nl}(r_2)Y_{lm}(\theta_2,\phi_2) = \left[\sum_i C_i e^{-A_i r_2} r_2^{l_i}\right] Y_{lm}(\theta_2,\phi_2), \quad l_i = 0,1,2,\cdots, \tag{4}$$

where C_i's are the normalization constants and A_i's are variational parameters. The parameters are then determined by optimizing the Rayleigh quotient $<\phi|h_1|\phi> / <\phi|\phi>$ with respect to α, β, γ so that E agrees with the experimental observation in vacuum [71, 72]. The potential (3) with positive sign is used to describe the interaction potential between the Li^+ core and the positron. That is, the positron-core interaction (in a.u.) is:

$$V_M^{(e^+)}(\vec{r}_1) = \frac{e^{-\mu r_1}}{r_1}\cos(\mu r_1)\left[1+2(e^{-2\alpha r_1}+\beta r_1 e^{-2\gamma r_1})\right], \tag{5}$$

where $\vec{r}_1$ denotes the coordinate of the positron with respect to the core. It is to be noted that the positron-core interaction seems to be a bit more repulsive than the real physical situation, as it takes care of the effect of exchange between the positron and the electron. Within this background, the non-relativistic Hamiltonian (in a.u.) of e^+Li under QP takes the form:

$$H = -\frac{1}{2}\nabla_1^2 - \frac{1}{2}\nabla_2^2 + V_M^{(e^+)}(\vec{r}_1) + V_M^{(e^-)}(\vec{r}_2) - \frac{e^{-r_{12}/\lambda_D}}{r_{12}}, \tag{6}$$

where $\vec{r}_{12} = \vec{r}_1 - \vec{r}_2$.

We now apply the SM to determine the resonance parameters - energy E_r and width Γ. The present SM has been extensively used by Ho and co-workers [73–77] to determine resonances

in atomic systems. In order to make the paper self-explanatory, here we just state the salient points of the method. Determining resonance parameters by the SM is based on the analysis of the spectral density $\rho(E)$, where $H\Psi = E\Psi$. In the Feshbach projection formalism, the spectral density of the states consists of two components - $\rho^P(E)$ and $\rho^Q(E)$, where P and Q are referred to the open space and close space respectively [77]. $\rho^P(E)$ is a smooth function of the energy E, whereas $\rho^Q(E)$ is a sequel of the complex poles of the Green's function concerned. For a real atomic system, $\rho^Q(E)$ can be obtained as [78]:

$$\rho^Q(E) = \frac{1}{\lambda_1 - \lambda_2} \int_{\lambda_1}^{\lambda_2} \rho_\lambda(E) d\lambda = \frac{1}{\lambda_1 - \lambda_2} \int_{\lambda_1}^{\lambda_2} \sum_i \delta(E_i(\lambda) - E) d\lambda, \tag{7}$$

where λ_1 and λ_2 respectively denote the maximum and minimum value of the scaling parameter λ included in the wavefunction Ψ. Using the properties of Dirac delta function, such as:

$$\int f(x)\delta(g - g(x))dx = f(x) \left[\frac{dg}{dx}\right]^{-1}_{g(x)=g},$$

equation (7) can further be simplified as:

$$\rho^Q(E) = \frac{1}{\lambda_1 - \lambda_2} \sum_i \left[\frac{dE_i(\lambda)}{d\lambda}\right]^{-1}_{E_i(\lambda)=E}. \tag{8}$$

Bowman [79] proved that for an isolated resonance equation (8) could be written in the following Lorentzian form:

$$\rho^Q(E) \cong x_0 + \frac{\triangle}{\pi} \frac{\Gamma/2}{(E - E_r)^2 + (\Gamma/2)^2}, \tag{9}$$

where x_0 is the baseline offset, $\triangle$ is the total area under the curve from the base line, E_r is the centre of the peak and Γ denotes the full width of the peak of the curve at half height (as shown in Figure 2).

In the present work, we use the following L^2 wavefunction:

$$\Psi(\vec{r}_1,\, \vec{r}_2;\, \lambda) = \sum_{i=1}^{N} \psi_i(r_1,\, r_2,\, r_{12},\, \lambda) = \sum_{l_i+m_i+n_i=0}^{\omega} C_{l_i m_i n_i}\, e^{-\lambda(r_1+r_2)} r_1^{l_i} r_2^{m_i} r_{12}^{n_i}, \tag{10}$$

where $C_{l_i m_i n_i}$ is linear expansion coefficient, and $l_i, m_i, n_i, \omega \in \mathbb{Z}^*$, the set of non-negative integers. ω determines the number of the terms in the wavefunction such that $\omega = 0$ stands for $N = 1$; $\omega = 1$ stands for $N = 4$; and so on. Energy levels of the Hamiltonian (6) for varying scaling parameter leads to the stabilization diagram (as shown in Figure 1). The density of the resonance state for the n-th energy level is given by:

$$\rho_n^Q(E) = \left[\frac{E_n(\lambda_{i+1}) - E_n(\lambda_{i-1})}{\lambda_{i+1} - \lambda_{i-1}}\right]^{-1}_{E_n(\lambda_i)=E}. \tag{11}$$

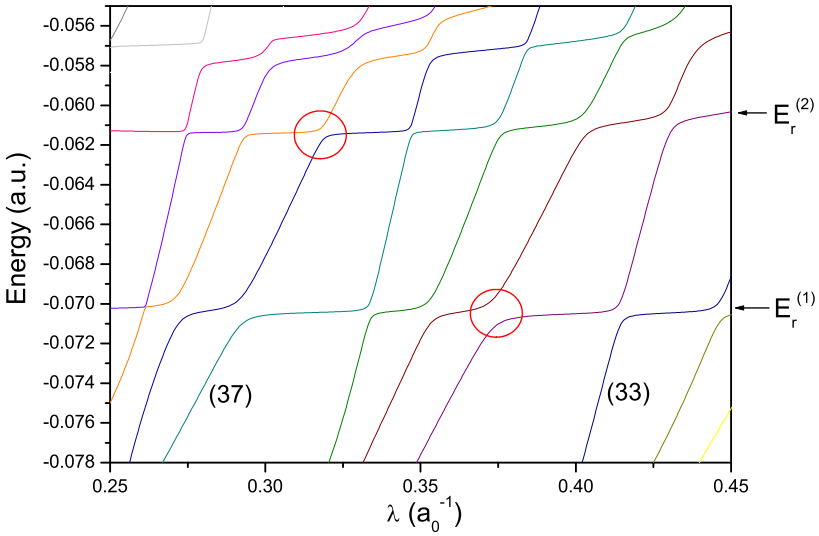

FIGURE 1. Stabilization plot for e^+Li embedded in QP for $\mu = 0.01$, obtained by using 680 terms ($\omega \leq 14$) in the wavefunction (10) and by giving the scaling parameter s an increment of 0.0005 units. The number in the parenthesis next to the solid line shows the order of appearance of the eigenvalues (energy levels). The arrows indicate the positions of resonances. The circles show the point of avoided crossing.

In general, E (and therefore $\rho_n^Q(E)$) changes slowly as a function of the λ. However, in certain cases, E varies rapidly in certain ranges of the scaling parameter (around an avoided crossing where the energy level takes rapid turn) causing $\rho_n^Q(E)$ to assume the form of a Lorentzian profile, like equation (9). We have calculated the density of resonance states $\rho_n^Q(E)$ for each pair of consecutive energy levels at the "avoided crossing" (shown in Figure 1). $\rho_n^Q(E)$ is then fitted with Lorentzian form (9) to obtain resonance energy E_r and resonance width Γ. Resonance parameters for that particular resonance are extracted from the best fitting (value of the "coefficient of determination" R^2 is closest to unity).

III. RESULTS AND DISCUSSION

We have determined the parameters α, β and γ by optimizing the Rayleigh quotient $< \phi|h_1|\phi > / < \phi|\phi >$ with respect to α, β, γ. The values of the parameters α, β and γ have been found as $\alpha = \beta = \gamma = 1.6559$. The binding energies of Li(ns) in QP along with the theoretical results and experimental observations in vacuum are shown in Table 1. From Table 1 it is apparent that our results of binding energies are in good accord with the theoretical results [67] and experimental observations [71, 72].

Figure 1 shows the stabilization diagram or stabilization plot (SP) for $\mu = 0.01$. This SP indicates the existence of two S-wave resonances below the $E_{th}^{Ps(2)}$. Energy and width of these resonances are computed by setting $N = 680$ ($\omega = 14$) in the wavefunction (10). Figure 2 shows the fittings of the density of states to the Lorentzian profile for some pairs of eigenvalues. Variation of the RP with the change in the pair of eigenvalues are shown in Table 2.

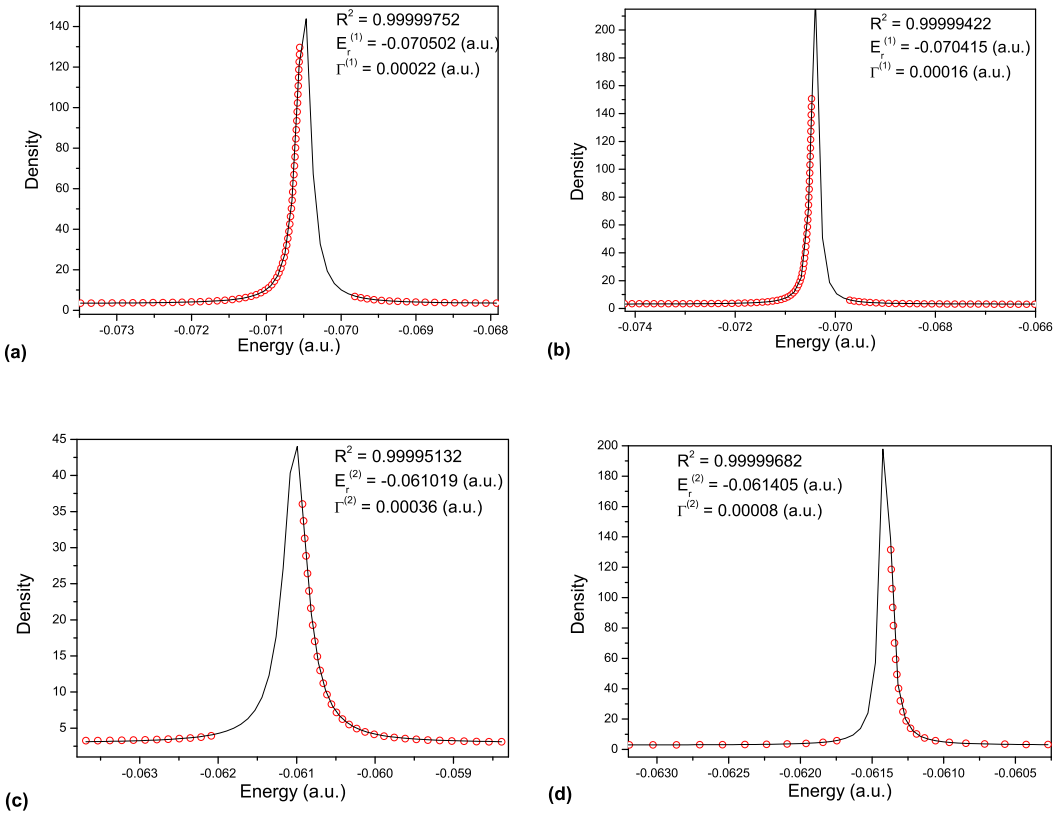

FIGURE 2. Fittings of the density of resonance states to the Lorentzian form for the lowest two resonances below the $Ps(n=2)$ threshold in e^+Li under QP for $\mu = 0.01$ The circles are the calculated values and the solid line is the fit function. (a) Fitting using $34th$ and $35th$ eigenvalues. (b) Fitting using $37th$ and $38th$ eigenvalues. (c) Fitting using $35th$ and $36th$ eigenvalues. (d) Fitting using $38th$ and $39th$ eigenvalues.

The convergence of the RP of the lowest S-wave resonance with increasing N in the wavefunction (10) is shown in Table 3. From this table it is seen that convergent results for the RP (up to three significant digits) can be obtained by considering N = 680 in the wavefunction (10). The uncertainty of our reported results is associated with the fourth significant digit. All reported results in this paper are calculated by setting N = 680 in the wavefunction (10). Also, the resonance energies are reported relative to the energy of the core. In Table 4, the energy and the width of the lowest two resonances in vacuum are compared with other available results. At this point, it is worthy to mention the effect of positron-core interaction on the final results. The interaction potential (5) takes account of the effect of exchange between the positron and the electron, so it is little more repulsive than the real one. But its effect is unduly small. We have checked this fact by considering other two model potentials representing positron-core interaction [70], which do not include the effect of exchange, namely:

$$V_M^{(e^+)}(\vec{r}_1) = \frac{e^{-\mu r_1}}{r_1}\cos(\mu r_1) \quad \text{and} \tag{12}$$

$$V_M^{(e^+)}(\vec{r}_1) = \frac{e^{-\mu r_1}}{r_1}\cos(\mu r_1)\left[1+2e^{-\varepsilon r_1}\right], \tag{13}$$

with $\varepsilon = 4.205$. The final result, that is the resonance parameters, is the same for all three

TABLE 1. Eigen energy, E (in a.u.), of Li(ns) embedded in QP relative to the energy of the core for various values of the screening parameter μ (in a_0^{-1}).

	States				
μ	2s	3s	4s	5s	6s
0.00	-0.198141	-0.074310	-0.038677	-0.023640	-0.015642
a:	-0.19815	-0.07415	-0.03862	-0.02364	-0.01595
b:	-0.19816	-0.07419	-0.03862	-0.02364	-0.01595
c:	-0.19814	-0.07418	-0.03862	-0.02364	-0.01594
0.01	-0.187938	-0.064299	-0.028785	-0.013947	-0.006158
0.02	-0.177768	-0.054491	-0.019549	-0.005793	
0.03	-0.167660	-0.045046	-0.011414	-0.000106	
0.04	-0.157643	-0.036094	-0.004735		
0.05	-0.147741	-0.027741			
0.06	-0.137976	-0.020084			
0.07	-0.128369	-0.013217			
0.08	-0.118938	-0.007254			
0.09	-0.109703	-0.002375			
0.10	-0.100678				

a: theoretical results of Laughlin and Victor [67]; b: Experimental results of Johansson [71]; c: experimental results of Bashkin and Stoner [72].

TABLE 2. R^2, $E_r^{(1)}$ (in a.u.) and $\Gamma^{(1)}$ (in a.u.) extracted from the fittings of the density of resonance states for different pair of consecutive energy levels at the avoided crossing to the Lorentzian profile for the lowest resonance below the Ps(n = 2) threshold in e^+Li under QP for $\mu = 0.01$. E_N denoted the eigenvalue number.

E_N	34 & 35	35 & 36	36 & 37	37 & 38
R^2	0.99999752	0.99996755	0.99997410	0.99999422
$-E_r^{(1)}$	0.070502	0.070399	0.070393	0.070415
$\Gamma^{(1)}$	0.00021584	0.00023617	0.00010589	0.00016179

TABLE 3. The lowest $S-$wave resonance energy and width below the $Ps(n=2)$ threshold in e^+Li embedded in QP.

	$-E_r^{(1)}$ (a.u.)			$\Gamma^{(1)}$ (a.u.)		
	$N=455$ $(\omega=12)$	$N=560$ $(\omega=13)$	$N=680$ $(\omega=14)$	$N=455$ $(\omega=12)$	$N=560$ $(\omega=13)$	$N=680$ $(\omega=14)$
$\mu=0.01$ (a_0^{-1})	0.070352	0.070406	0.070502	0.00024568	0.00019412	0.00021584
$\mu=0.02$ (a_0^{-1})	0.060224	0.060278	0.060380	0.00024038	0.0001948	0.0002184

cases. Note that the potential $V_M^{(e^+)}$ seen by the positron is simply the electrostatic potential of the nucleus and of core electrons. In case of potential (12), it is assumed that all the charges are concentrated at the nucleus; whereas in case of potential (13), it is assumed that the nuclear charge is screened by the 1s electrons. Since, at low energies a positron cannot penetrate into the core region, all the three potentials are reasonably good for approximating positron-core interaction.

In Table 5, the energy and the width of the lowest two resonances below the $E_{th}^{Ps(2)}$ are put up for various values of the screening parameter of QP. For comparison, results in DP are

TABLE 4. Comparison of the energy (a.u.) and the width (a.u.) of the lowest two S-wave resonance states below the $Ps(n=2)$ threshold in e^+Li in vacuum. Column (A): results of Ward *et al* [57], Column (B): results of Roy and Ho [59], (C): results of Han *et al* [52], Column (D): CC5 results of Liu *et al* [51], Column (E): Results of Umair and Jonsell for MP1 [44], Column (F): results of Yamashita and Kino for model potential V [45].

	Present	(A)	(B)	(C)	(D)	(E)	(F)
$-E_r^{(1)}$ (a.u.)	0.080550	0.087526	0.80690	0.080658	0.087305	0.080624	0.080643
$\Gamma^{(1)}$(a.u.)	0.00022	0.00147	0.00021	0.00020*	0.00276	0.00023	0.00013
$-E_r^{(2)}$ (a.u.)	0.071436	0.07448	0.072532	0.073932	0.074112		
$\Gamma^{(2)}$(a.u.)	0.00008	0.00004	0.00008	0.00004	0.00096		

*this number is taken from the text of Han *et al* [52]. The number reported by them in TABLE I is 2.93 eV.

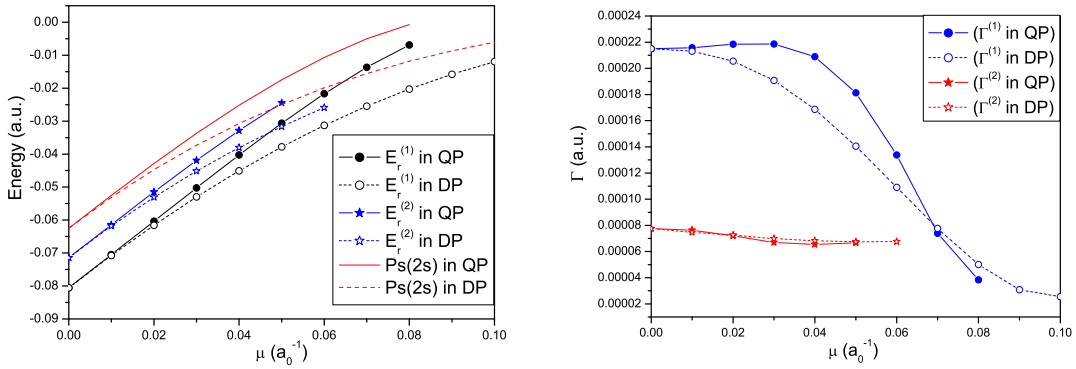

FIGURE 3. (a) The lowest two resonance energies, $E_r^{(1)}$ and $E_r^{(2)}$, below the $Ps(n=2)$ threshold in e^+Li embedded in plasmas for different values of the plasma screening parameter μ. (b) Resonance widths, $\Gamma^{(1)}$ and $\Gamma^{(2)}$, corresponding to the resonance energies in (a) for different values of the plasma screening parameter μ.

also included in that table. Graphical representation of the RP are made in Figure 3. From Table 5 and Figure 3, we note that the effect of increasing plasma screening strength is to push the resonance energy towards the energy of Ps(2s). It is rather fast in QP than in DP. It is expected, as the screened potentials become weaker with increasing screening effect. Furthermore, for a particular value of μ, DHCP is weaker than DHP. The variation of the resonance width with increasing μ is interesting. The variation of the resonance width of the second resonance is almost the same in the two different plasmas. But, with increasing μ the width of the lowest resonance in QP increases slightly at first and then starts decreasing rapidly. Whereas in DP, with increasing screening effect at first it decreases slowly and then it starts decreasing rapidly. It is not difficult to understand qualitatively the reason behind such behaviour. Note that this is a Feshbach-type resonance which is formed owing to motion of an excited positronium in the field of a positively charged ion (Li^+) [82]. In general, with increasing screening effect, the width of a Feshbach resonance decreases. This is due to the movement of charged particles being slower, which leads to increasing lifetime of such a resonance state. Thus, the resonance width becomes narrower as a consequence of the uncertainty principle [80, 81]. The enhancement of width in QP for small screening effects might be owing to the combined effect of oscillatory behaviour of the DHCP, and the equality of the attractive and repulsive force in positron-lithium system. The increase of width in QP for small screening effects were also observed in a number of earlier investigations [1, 2, 8, 73].

TABLE 5. Energy (a.u.) and width (a.u.) of the lowest two $S-$wave resonance states below the $Ps(n=2)$ threshold in e^+Li embedded in plasmas for various values of the plasma screening parameter μ.

	Energy (a.u.)				Width (a.u.)			
μ	$-E_r^{(1)}$ (a.u.)		$-E_r^{(2)}$ (a.u.)		$\Gamma^{(1)}$ (a.u.)		$\Gamma^{(2)}$ (a.u.)	
(a_0^{-1})	QP	DP	QP	DP	QP	DP	QP	DP
0.00	-0.080550	-0.080550	-0.071436	-0.071436	0.000215	0.000215	0.000078	0.000078
0.01	-0.070502	-0.070781	-0.061405	-0.061824	0.000216	0.000213	0.000076	0.000075
0.02	-0.060380	-0.061576	-0.051490	-0.053069	0.000218	0.000206	0.000072	0.000072
0.03	-0.050245	-0.052992	-0.041913	-0.045154	0.000218	0.000191	0.000067	0.000070
0.04	-0.040262	-0.045068	-0.032863	-0.038031	0.000209	0.000169	0.000065	0.000068
0.05	-0.030658	-0.037827	-0.024441	-0.031643	0.000181	0.000140	0.000067	0.000068
0.06	-0.021702	-0.031284		-0.025934	0.000134	0.000109		0.000068
0.07	-0.071368	-0.025440			0.000074	0.000078		
0.08	-0.006876	-0.020287			0.000038	0.000050		
0.09		-0.015806				0.000031		
0.10		-0.011968				0.000026		

IV. CONCLUSIONS

In conclusion, we have found two Feshbach resonances in e^+Li embedded in QP lying below the $E_{th}^{Ps(2)}$. The appearance of these resonances predicts the positron-lithium bound system in QP. The position of the resonances are shifted towards the Ps(2s) with increasing strength of plasma screening. The width of the lowest resonance increases slowly for small screening effect, but decreases rapidly for strong screening effect. This particular behaviour is not found in classical Debye-type plasmas. Recently, motivating experiments have been performed to search for resonances in atomic systems involving positrons in vacuum [83, 84]. We hope that our present investigation will stimulate an experimental search for resonances in the positron-lithium system under plasma environments.

ACKNOWLEDGMENTS

The work was supported by the Ministry of Science and Technology of the ROC. Arijit Ghoshal sincerely acknowledge the support received from UGC through Major Research project (F. No. 43-415/2014(SR)).

REFERENCES

1. A. Ghoshal and Y. K. Ho, *J. Phys. B* **50**, 075001 (2017).
2. A. Ghoshal and Y. K. Ho, *Few-Body. Syst.* **58**, 138 (2017).
3. P. Jiang, Z. Jiang, and S. Kar, *F. Body. Syst.* **57**, 1165 (2016).
4. Z. Jiang, Y.-Z. Zhang, and S. Kar, *Phys. Plasmas* **22**, 052105 (2015).
5. P. K. Shukla and M. Akbari-Moghanjoughi, *Phys. Rev. E* **87**, 043106 (2013).
6. S. A. Khana and and Z. Wazir, *Chin. Phys. B* **22**, 025201 (2013).

7. B. Eliasson and P. K. Shukla, *Plasma and Fusion Research: Review Articles* **4**, 032 (2009).
8. A. Ghoshal and Y. K. Ho, *J. Phys. B* **42**, 075002 (2009); *J. Phys. B* **42**, 175006 (2009); *Phys. Plasmas* **16**, 073302 (2009); *Comp. Phys. Comm.* **182**, 122 (2011).
9. S. Ali, N. Shukla, and P. K. Shukla, *Europhys. Lett.* **78**, 45001 (2007).
10. S. Ali and P. K. Shukla, *Phys. Plasmas* **13**, 052113 (2006).
11. P. K. Shukla and B. Eliasson, *Phys. Rev. Lett.* **96**, 245001 (2006).
12. F. Haas, L. G. Garcia, J. Goedert, and G. Manfredi, *Phys. Plasmas* **10**, 3858 (2003).
13. P. Rej and A. Ghoshal, *Phys. Plasmas* **24**, 043506 (2017).
14. J. Daligault, *Phys. Plasmas* **23**, 032706 (2016).
15. R. K. Janev, S. Zhang, and J. Wang *Matter Radiat. Extrem.* **1**, 237 (2016).
16. D. Jakimovski, N. Markovska and R. K. Janev *J. Phys. B* **49**, 205701 (2016).
17. P. Rej and A. Ghoshal, *Phys. Plasmas* **21**, 113509 (2014).
18. S. Son, *Phys. Plasmas* **21**, 034502 (2014).
19. S. Nayek and A. Ghoshal, *Phys. Scr.* **88**, 045301 (2013).
20. L. Y. Zhang, X. Qi, X.Y. Zhao, D. Y. Meng, G. Q. Xiao, W. S. Duan, and L. Yang, *Phys. Plasmas* **20**, 113301 (2013).
21. A. Bhattacharya, M. Z. M. Kamali, A. Ghoshal, and K. Ratnavelu, *Phys. Plasmas* **20**, 083514 (2013).
22. A. Ghoshal and Y. K. Ho, *Chin. J. Phys.* **48**, 747 (2010).
23. D. H. Ki and Y. D. Jung, *Phys. Plasmas* **17**, 074506 (2010).
24. Y. H. Koo and Y. D. Jung, *Z. Naturforsch.* **64a**, 237 (2009).
25. V. N. Tsytovich, *Astroparticle Phys.* **5**, 285 (1996).
26. Y. D. Jung, *Phys. Plasmas* **8**, 3842 (2001).
27. G. Chabrier, F. Douchin, and A. Y. Potekhin, *J. Phys. Condens. Matter* **14**, 9133 (2002).
28. D. Kremp, M. Schlanges, and W. D. Kraft, *Quantum Statistics of Nonideal Plasmas* (Springer, Berlin, 2005).
29. A. V. Andreev, *JETP Lett.* **72**, 238 (2000).
30. M. Marklund and P. K. Shukla, *Rev. Mod. Phys.* **78**, 591 (2006).
31. P. A. Markowich, C. A. Ringhofer, and C. Schmeiser, *Semiconductor Equations* (Springer-Verlag, New York, 1990).
32. G. V. Shpatakovskaya, *J. Exp. Theor. Phys.* **102**, 466 (2006).
33. L. Wei and Y N Wang, *Phys. Rev. B* **75**, 193407 (2007).
34. L. K. Ang, W. S. Koh, Y. Y. Lau, and T. J. T. Kwan, *Phys. Plasmas* **13**, 056701 (2006).
35. D. E. Chang, A. S. Sorensen, P. R. Hemmer, and M. D. Lukin, *Phys. Rev. Lett.* **97**, 053002 (2006).
36. T. C. Killian, *Nature (London)* **441**, 298 (2006).
37. K. Becker, K. Koutsospyros, S. M. Yin, C. Christodoulatos, N. Abramzon, J. C. Joaquin, and G. Brelles-Marinoet, *Plasma Phys. Control. Fusion* **47**, B513 (2005).
38. S. C. Na and Y. D. Jung, *Phys. Lett. A* **372**, 5605 (2008).
39. G. Manfredi, *Fields Inst. Commun.* **46**, 263 (2005).
40. P. K. Shukla, B. Eliasson, *Phys. Lett. A* **372**, 2897 (2008).
41. D. Bressanini, *Phys. Rev. Lett.* **109**, 223401 (2012).
42. J. Mitroy, *Phys. Rev. A* **70**, 024502 (2004).
43. A. Ghoshal and Y. K. Ho, *Phys. Rev. A* **95**, 052502 (2017).

44. M. Umair and S. Jonsell, *Phys. Rev. A* **93**, 052707 (2016).
45. T. Yamashita and Y. Kino, *Euro. Phys. J. D* **70**, 190 (2016).
46. M. Umair and S. Jonsell, *J. Phys. B* **49**, 015004 (2016).
47. M. Umair and S. Jonsell, *Phys. Rev. A* **92**, 012706 (2015).
48. J. Mitroy and J. Grineviciute, *Phys. Rev. A* **88**, 022710 (2013).
49. R.-M. Yu, Y.-J. Cheng, W. Yang, and Y.-J. Zhou, *Chin. Phys. B* **21**, 053402 (2012).
50. J. R. Machacek, R. Boadle, S. J. Buckman, and J. P. Sullivan, *Phys. Rev. A* **86**, 064702 (2012).
51. F. Liu, Y. Cheng, Y. Zhou, and L. Jiao, *Phys. Rev. A* **83**, 032718 (2011).
52. H. Han, Z. Zhong, X. Zhang, and T. Shi, *Phys. Rev. A* **78**, 044701 (2008).
53. Y. K. Ho, *Nuclear Instruments and Methods in Physics Research B* **266** 516 (2008).
54. M. W. J. Bromley and J. Mitroy, *Phys. Rev. A* **73**, 032507 (2006).
55. J. Mitroy, *Phys. Rev. Lett.* **94**, 033402 (2005).
56. S. Kar and Y. K. Ho, *Euro. Phys. J. D* **35**, 453 (2005).
57. S. J. Ward, M. Horbatschz, R. P. McEachran, and A. D. Stauffer, *J. Phys. B* **22**, 3763 (1989).
58. U. Roy, Y. K. Ho, *Nuclear Instruments and Methods in Physics Research B* **221**, 36 (2004).
59. U. Roy and Y. K. Ho, *J. Phys. B* **35**, 2149 (2002).
60. J. Mitroy, M. W. J. Bromley, and G. G. Ryzhikh, *J. Phys. B* **35**, R81 (2002).
61. E. Surdutovich, J. M. Johnson, W. E. Kauppila, C. K. Kwan, and T. S. Stein, *Phys. Rev. A* **65**, 032713 (2002).
62. T. S. Stein, M. Harte, J. Jiang, W. E. Kauppila, C. K. Kwan, H. Li, and S. Zhou, *Nucl. Instrum. Methods Phys. Res. Sect. B* **143**, 68 (1998).
63. Z. Wang, P. Winkler, and B. T. Pickup, *Chem. Phys.* **135**, 247 (1989).
64. M. A. Moghanjoughi, *Phys. Plasmas* **20**, 102115 (2013).
65. P. K. Shukla, B. Eliasson, *Phys. Rev. Lett.* **108**, 165007 (2012).
66. A. Hilbert, *Adv. At. Mol. Phys.* **18**, 309 (1982).
67. C. Laughlin and G. A. Victor, *Adv. At. Mol. Phys.* **25**, 163 (1988).
68. Y. P. Varshni, *Phys. Rev. A* **38**, 1595 (1988).
69. Y. P. Varshni, *Eur. Phys. J. D* **22**, 229 (2003).
70. P. Cavaliere and G. Ferrante, *NUOVO CIMENTO* **14B**, 127 (1973).
71. I. Johansson, *Ark. Fys.* **15**, 169 (1959).
72. S. Bashkin and J. O. Stoner, in Atomic Energy Levels and Gotrian Diagrams vol 1 (Amsterdam: North-Holland) (1975).
73. A. Ghoshal and Y. K. Ho, *Euro. Phys. J. D* **56**, 151 (2010).
74. A. Ghoshal and Y. K. Ho, *Phys. Rev. A.* **79**, 062514 (2009).
75. A. Ghoshal and Y. K. Ho, *Few-Body Syst.* **46**, 249 (2009).
76. T. K. Fang and Y. K. Ho, *J. Phys. B* **32**, 3863 (1999).
77. S. S. Tan and Y. K. Ho, *Chin. J. Phys.* **35**, 701 (1997).
78. J. Muller, X. Yang, and J. Burgdorfer, *Phys. Rev. A* **49**, 2470 (1994).
79. J. M. Bowman, *J. Phys. Chem.* **90**, 3492 (1986).
80. Y. Ning, Z. C. Yan, and Y. K. Ho, *Phys. Plasmas* **22**, 013302 (2015).
81. Y. Ning, Z. C. Yan, and Y. K. Ho, *Atoms* **4**, 3 (2016).
82. Y. K. Ho, *Phys. Rev. A* **38**, 6424 (1988).

83. A. P. Mills Jr., *Can. J. Phys.* **91**, 751 (2013).
84. K. Michishio, T. Kanai, S. Kuma, T. Azuma, K. Wada, I. Mochizuki, T. Hyodo, A. Yagishita, and Y. Nagashima, *Nature Communications* 7:11060 [DOI: 10.1038/ncomms11060].